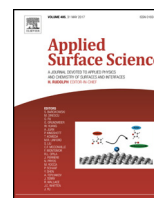




Contents lists available at ScienceDirect

Applied Surface Science

journal homepage: [www.elsevier.com/locate/apsusc](http://www.elsevier.com/locate/apsusc)

Full length article

# Controlling the optical parameters of self-assembled silver films with wetting layers and annealing

Arkadiusz Ciesielski<sup>a,\*</sup>, Lukasz Skowronski<sup>b</sup>, Marek Trzcinski<sup>b</sup>, Tomasz Szoplík<sup>a</sup><sup>a</sup> University of Warsaw, Faculty of Physics, Pasteura 7 Str., 02-093 Warsaw, Poland<sup>b</sup> UTP University of Science and Technology, Institute of Mathematics and Physics, Kaliskiego 7 Str., 85-796 Bydgoszcz, Poland

## ARTICLE INFO

## Article history:

Received 30 July 2016

Received in revised form 4 January 2017

Accepted 5 January 2017

Available online xxx

## Keywords:

Silver

Thin films

Self-assembly

Permittivity, ellipsometry

Percolation

Wetting layers

Annealing

Segregation

## ABSTRACT

We investigated the influence of presence of Ni and Ge wetting layers as well as annealing on the permittivity of Ag films with thicknesses of 20, 35 and 65 nm. Most of the research on thin silver films deals with very small (<20 nm) or relatively large (≥50 nm) thicknesses. We studied the transition region (around 30 nm) from charge percolation pathways to fully continuous films and compared the values of optical parameters among silver layers with at least one fixed attribute (thickness, wetting and capping material, post-process annealing). Our study, based on atomic force microscopy, ellipsometric and X-ray photoelectron spectroscopy measurements, shows that utilizing a wetting layer is comparable to increasing the thickness of the silver film. Both operations decrease the roughness-to-thickness ratio, thus decreasing the scattering losses and both narrow the Lorentz-shaped interband transition peak. However, while increasing silver thickness increases absorption on the free carriers, the use of wetting layers influences the self-assembled internal structure of silver films in such a way, that the free carrier absorption decreases. Wetting layers also introduce additional contributions from effects like segregation or diffusion, which evolve in time and due to annealing.

© 2017 Published by Elsevier B.V.

## 1. Introduction

Thin silver films are used in sensor, plasmonic and metamaterial applications, provided that they have low both scattering and ohmic losses [1–14]. Scattering losses are reduced in metal layers if evaporated on polished substrates with low roughness (achievable value for SiO<sub>2</sub> is 0.3 nm roughness root mean square – RMS). Even better results can be achieved when the use of wetting layer promotes adhesion between metal particles and the substrate and thus prevents island growth. To block the Volmer-Weber growth, a number of wetting interlayers, like Ge, Ni, Ti, Cr or Cu were introduced [2–4,7,9–14]. The seed layer approach leads to the reduction of the surface roughness of deposited films and allows to acquire continuous Ag layers, even if the thickness is lower than 30 nm. RMS surface roughness of 10 nm-thick Ag films equals only 0.4; 0.9; and 2.0 nm for Ge, Ni and Ti wetting layers, respectively [10]. Germanium wetting layer is the most efficient in reduction of scattering losses by smoothing the surface of silver films due to greater adhesion of Ag to Ge than that of Ag to fused silica – it causes low Ag adatom surface diffusivity [8]. However, this high adhesion of Ge to Ag also

induces segregation of Ge atoms into Ag grain boundaries as well as film free surface. That results in a considerable increase of specific resistivity and limits the potential use of Ag films deposited on Ge wetting layer in plasmonic applications [13]. Moreover, the use of a segregating material may introduce new bands to the permittivity of a silver system, while increasing or decreasing the primary ones [13,14]. These new contributions may be tailored by temperature treatment (e.g. cooling the substrate in the deposition process) or the use of capping layers of another segregating material, such as Al<sub>2</sub>O<sub>3</sub> [13].

In this work, we discuss the influence over time of wetting layers on the crystallinity-induced permittivity of silver films with different thicknesses. Application of annealing allowed to control the self-assembly of the silver layers and in turn the additional contributions from the wetting films. The undesired influence of wetting on the primary permittivity components, like the Drude-Lorentz free carrier absorption, could also be mitigated. We chose to examine the permittivity of 20 and 35 nm-thick silver layers since this thickness range is not yet fully investigated. For the first wetting layer, we chose Ni, because of the good smoothing performance and minimal impact on the low-frequency resistivity [10] as well as weak solubility in silver [15]. For the second wetting layer, we chose Ge because of excellent smoothing performance [2] and the fact that it is most commonly used. For protection against cor-

\* Corresponding author.

E-mail address: [aciesiel@igf.fuw.edu.pl](mailto:aciesiel@igf.fuw.edu.pl) (A. Ciesielski).

rosion we chose LiF to serve as capping layer, since it is easy to sputter and, unlike  $\text{Al}_2\text{O}_3$  exhibits no segregation in silver.

The permittivity values of silver most commonly employed in contemporary numerical simulations (e.g. [16–18]) are usually the ones determined by Johnson & Christy [19] or in the papers collected by Palik [20] and do not comprehend the vast range of Ag films grown in different ways. Even more recent attempts to re-evaluate the dielectric function of silver focus either on discontinuous layers with thicknesses below 20 nm [1,21–23], fully continuous layers with thicknesses 100 nm or greater [24,25] or investigate similar to the ones already researched in order to evaluate the correctness of previous results [26]. However, in case of silver layers grown on wetting films, only the permittivity values for Ag grown on Au nanoparticles have been reported [27]. Here we provide silver permittivity values for use in simulations of silver grown on  $\text{SiO}_2$  substrates with Ge or Ni interlayers.

## 2. Materials and methods

All films were deposited from fabmate or tungsten crucibles using PVD75 Lesker e-beam evaporator, on fused silica substrates with RMS roughness equal to 0.3 nm. The purity of the evaporation materials was 4N for silver, 4.5N for nickel, 5N for germanium and 3N for LiF. Before evaporation, substrates were cleaned with argon flow at 2 bar pressure. Ni and Ge were evaporated at an average deposition rate of 0.5 Å/s to form a 2 nm-thick wetting layer. Silver films of thickness 20, 35, and 65 nm were evaporated at an average deposition rate of 2 Å/s either directly on  $\text{SiO}_2$  substrates or on Ge or Ni wetting interlayers. LiF was evaporated at an average deposition rate of 1 Å/s to form a 3 nm-thick capping layer. Deposition rate and total film thickness were monitored by two quartz weights inside the deposition chamber. Then, film thicknesses were verified by Dektak 6M stylus profiler. The pressure in the vacuum chamber was kept below  $5 \times 10^{-5}$  Torr during the whole deposition process. The crucible-substrate distance was 40 cm.

Roughness measurements were performed using NT-MDT and AIST-NT atomic force microscopes (AFM). The values of roughness RMS as well as average surface grain size were determined using Gwyddion (<http://gwyddion.net>) software.

Ellipsometric azimuths  $\Psi$  and  $\Delta$  of fabricated samples were measured in the UV–VIS–MIR spectral range (0.06–6.5 eV) for three angles of incidence (65°, 70° and 75°) by the use of two instruments: V-VASE (J.A. Woollam Co., Inc.) in the UV–VIS–NIR and Sendira (Sentech GmbH) in the MIR. The complex dielectric functions of Ag layers were extracted using a layered model of the samples. The optical constants of the Ni wetting layer were determined in a separate experiment. Ge atoms exhibit intense segregation in silver films, therefore no independent Ge layer was considered in the model. The permittivities of silver films were then interpreted in terms of the Lorentz, Drude-Lorentz and Cody-Lorentz oscillator models. The Cody-Lorentz oscillator is commonly used to model the permittivity of semiconductors, however, the shape of modified Lorentz oscillator used by Rioux et al. [28] to reproduce the permittivity of silver at wavelengths below 320 nm is very similar to the Cody-Lorentz shape. Hence, the Cody-Lorentz oscillator was used here in conjunction with an additional tiny Lorentz oscillator to model the permittivity of silver below 320 nm. The differences in the values of permittivity obtained using both models are negligible except for wavelengths shorter than 250 nm, where the  $\Psi$  and  $\Delta$  azimuths are subject to large noise, but even so, the discrepancy is rather small (see Fig. S1 in the Supporting information for details). Electron energy loss function (LF) was calculated from the permittivity values using the following formula:  $\text{LF} = -\text{Im}(\varepsilon^{-1})$ , where  $\varepsilon$  is the complex permittivity of the layer.

The XPS measurements were performed at base pressure  $\leq 2 \cdot 10^{-10}$  mbar. Monochromatic radiation from Al K $\alpha$  source ( $\hbar\omega = 1486.6$  eV) was used to excite photoelectrons, the incidence angle was 55°. Photoemission spectra were recorded using VG Scienta R3000 hemispherical analyser oriented perpendicular to the samples' surface. The XPS data were recorded from all of the elements found at the surface with the energy resolution set to 100 meV with the exception of lithium. The XPS data recordings were interlaced by Ar ion etching in order to study the chemical composition of subsequent sublayers. The energy of Ar ions was 4 keV and the incidence angle was 69°. Ion beam scanned the area of  $4 \times 4$  mm in order to etch the analysed surface homogeneously. The concentrations of elements were estimated by fitting the most intensive peaks to Gauss-Lorentz shapes by using CasaXPS® software.

## 3. Results and discussion

### 3.1. Dependence of Ag film permittivity on thickness and roughness

Fig. 1 presents real (a) and imaginary (b) parts of permittivity of 20 and 35 nm-thick silver films in comparison to those of a fully continuous 65 nm-thick film. The most distinctive discrepancy is observed in the Lorentz-shaped peak in the imaginary part as well as the Drude term present in both real and imaginary parts. In most papers, e.g. [29,30], the Lorentz-shaped peak is attributed to the interband transitions at the L point in the Brillouin zone. However, while most theoretical approaches can predict the existence of this peak, none of them is able to exactly determine its value. In our case, for the thinnest, 20 nm-thick layer, the Lorentz-shaped band is centered at 378 nm and with the increase of silver thickness, a blueshift of this band is observed. Furthermore, the band gets narrower and the value of the maximum diminishes – from 0.75 in the case of 20 nm-thick film to 0.4 for the 65 nm-thick film. This correlates to the RMS-to-thickness ratio presented in Table 1. For the 20 nm film, the RMS-to-thickness ratio is most profound, implying that a large part of the layer is composed of narrow hills, where energy bands are sparse and shifted with respect to those of the bulk material. This also indicates an additional contribution from the intraband transitions. Moreover, those narrow hills increase the range of wavevectors accessible to surface plasmon-polaritons (SPP), allowing light to be coupled into SPP waves. Thus we interpret that the shape of the Lorentz band is intrinsically connected to the RMS-to-thickness ratio and originates not only from the contribution of the interband transitions at the L point in the Brillouin zone, but also from the intraband transitions as well as surface plasmon-polariton excitations. For thicker layers, the RMS-to-thickness ratio is lower and thus intraband transitions and localized plasmon coupling are limited. This results in narrowing and diminishing of the Lorentz-shaped band. For the 65-nm thick layer, the peak is barely observable, but on the other hand the maximum value of the Cody-Lorentz-shaped peak centered at 277 nm increased from 3.52 to 3.79. This suggests, that for very thick layers, the band structure at the L point resembles the band structure at other points in the Brillouin zone, at which the interband transitions contribute to Cody-Lorentz-shaped peak. We believe, however, that this is not strictly connected to the layer thickness, but rather to the RMS-to-thickness ratio corresponding to crystallinity.

To further investigate the impact of Ag roughness on the values of permittivity, we have used the RMS parameter of the 20 nm-thick silver film to split the silver film in the theoretical model into two sublayers. The top sublayer with triangular periodic roughness of height equal to the RMS value incorporates air to an intermix layer with silver content of 50% (the Bruggeman Effective Medium

Download English Version:

<https://daneshyari.com/en/article/5347705>

Download Persian Version:

<https://daneshyari.com/article/5347705>

[Daneshyari.com](https://daneshyari.com)